

SURFACE WAVES IN SOLAR GRANULATION OBSERVED WITH SUNRISE

M. ROTH¹, M. FRANZ¹, N. BELLO GONZÁLEZ¹, V. MARTÍNEZ PILLET², J. A. BONET², A. GANDORFER³, P. BARTHOL³,
S. K. SOLANKI^{3,4}, T. BERKEFELD¹, W. SCHMIDT¹, J. C. DEL TORO INIESTA⁵, V. DOMINGO⁶, AND M. KNÖLKER⁷

¹ Kiepenheuer-Institut für Sonnenphysik, Schöneckstr. 6, 79104 Freiburg, Germany; mroth@kis.uni-freiburg.de

² Instituto de Astrofísica de Canarias, C/Vía Láctea s/n, 38200 La Laguna, Tenerife, Spain

³ Max-Planck-Institut für Sonnensystemforschung, Max-Planck-Str. 2, 37191 Katlenburg-Lindau, Germany

⁴ School of Space Research, Kyung Hee University, Yongin, Gyeonggi 446-701, Republic of Korea

⁵ Instituto de Astrofísica de Andalucía (CSIC), Apartado de Correos 3004, 18080 Granada, Spain

⁶ Grupo de Astronomía y Ciencias del Espacio, Universidad de Valencia, 46980 Paterna, Valencia, Spain

⁷ High Altitude Observatory, National Center for Atmospheric Research, P.O. Box 3000, Boulder, CO 80307-3000, USA

Received 2010 June 16; accepted 2010 August 6; published 2010 October 15

ABSTRACT

Solar oscillations are expected to be excited by turbulent flows in the intergranular lanes near the solar surface. Time series recorded by the IMAx instrument on board the SUNRISE observatory reveal solar oscillations at high spatial resolution, which allow the study of the properties of oscillations with short wavelengths. We analyze two time series with synchronous recordings of Doppler velocity and continuum intensity images with durations of 32 minutes and 23 minutes, respectively, recorded close to the disk center of the Sun to study the propagation and excitation of solar acoustic oscillations. In the Doppler velocity data, both the standing acoustic waves and the short-lived, high-degree running waves are visible. The standing waves are visible as temporary enhancements of the amplitudes of the large-scale velocity field due to the stochastic superposition of the acoustic waves. We focus on the high-degree small-scale waves by suitable filtering in the Fourier domain. Investigating the propagation and excitation of f - and p_1 -modes with wavenumbers $k > 1.4 \text{ Mm}^{-1}$, we also find that exploding granules contribute to the excitation of solar p -modes in addition to the contribution of intergranular lanes.

Key words: Sun: granulation – Sun: helioseismology – Sun: photosphere – waves

1. INTRODUCTION

Solar p -modes are believed to be stochastically excited in the near surface layers of the Sun by turbulent convection. The process can be described as acoustic radiation by turbulent multipole sources (Unno 1964). Further theoretical descriptions of the excitation of solar oscillations follow the work on stochastic driving by turbulent convection presented by Goldreich & Keeley (1977) and Goldreich & Kumar (1988). These models were successful in explaining the acoustic power distribution over a wide range in frequencies as is manifested in the ensemble of solar p -modes.

Numerical simulations of convection, as described, e.g., by Nordlund (1985) or Stein & Nordlund (2001), predict supersonic downdrafts which could play a role in the excitation of the solar oscillations. Actually, the turbulent velocity field from the numerical simulations by Stein & Nordlund (2001) was used by Samadi et al. (2003) to determine the energy supply rate of convection into the solar oscillations.

For the seismology of the Sun and Sun-like stars, knowledge of the stochastic properties of the source function that drives p -modes would be a valuable input. In local helioseismology, e.g., the sensitivity functions which connect the acoustic properties of the p -modes with physical quantities in the Sun depend on the source function whose properties are not known and must be estimated (Birch et al. 2004). In addition, the Sun could serve as a paradigm for stellar seismology since the interaction of pulsations and convection and the energy gain and loss of p -modes from radiation and convection is a general problem of stellar physics (Houdek 2006).

When searching for the possible locations of the wave sources on the Sun, the turbulent downdrafts in the dark intergranular lanes are primary targets. So-called acoustic events, which are individual sunquakes with epicenters near the solar surface

and located in the intergranular lanes, are assumed to feed continuously energy into the resonant p -modes of the Sun. Studies of such acoustic events were carried out by Rimmele et al. (1995) and Goode et al. (1998) with the result that such events have typical durations of 5 minutes and are caused by collapsing intergranular lanes.

In this contribution, our basis for further studies of the driving of the solar oscillations are Dopplergrams of the velocity above the solar surface. Time series recorded with the Imaging Magnetograph eXperiment (IMaX) instrument (Martínez Pillet et al. 2010) on board the balloon-borne observatory SUNRISE (Solanki et al. 2010; Barthol et al. 2010) provide the spatial and temporal resolution needed to measure the propagation of acoustic oscillations in the granules and the intergranular lanes. We assume that acoustic events could be observed as they eventually cause waves to propagate away from the location of the source. The unprecedented spatial resolution of the data makes it worthwhile to study the excitation and propagation of acoustic waves visible in the solar photosphere. As a new result, we find that the acoustic power is not only enhanced in the intergranular lanes and along the borders of the granules but also above large granules, where splitting processes are about to occur. Surprisingly, the excitation of waves of high wavenumber seems to be a diagnostic of pending granule splitting.

2. OBSERVATION AND DATA REDUCTION

For our study, we use a time series of solar granulation with a field of view (FOV) of $51''5 \times 51''5$ located close to the disk center. The data were obtained with IMaX (Martínez Pillet et al. 2010) on board the SUNRISE balloon-borne solar observatory (Solanki et al. 2010; Barthol et al. 2010) between 00:35:49 UT and 00:59:57 UT (1st series) and 01:30:41 UT and 02:02:48 UT on 2009 June 9 (2nd series). The IMaX instrument and the

reduction process that was applied to the data are described in detail in Martínez Pillet et al. (2010) and shall be briefly summarized in the following.

The IMAx filtergraph was operated in the V5-6 observing mode, recording all Stokes parameters at $\lambda = [\pm 80, \pm 40, +227]$ mÅ with respect to the line center of Fe I 5250.2 Å ($g_{\text{eff}} = 3$, $\chi = 0.121$ eV). The exposure time for a picture at a single wavelength position was 6 s, while the entire line was scanned in 33 s.

In the data reduction process, the dark current was removed, and a flat-field procedure damped residual impurities, i.e., dust particles or scratches. In addition, the interference fringes—caused by the polarizing beam splitter—were removed from the images by attenuating their contribution in Fourier space. Furthermore, a spatially dependent blueshift over the FOV was calibrated and removed. Phase-diversity measurements that were recorded close in time to the actual data, were used to reconstruct all pictures. The corrected images of the two cameras were merged to increase the signal-to-noise ratio which is of the order of 4×10^2 , related to the continuum intensity (I_c) in the reconstructed data. In a last step, cross talk induced by residual motion was removed. Thus, we obtained time series with lengths of 24 and 32 minutes, respectively, and a cadence of 33 s. A spatial resolution between 0'.15 and 0'.18 was achieved by combining the on-board image stabilization system (Gandorfer et al. 2010; Berkefeld et al. 2010; Martínez Pillet et al. 2010).

Besides Doppler velocity (v_{Dopp}) and continuum intensity (I_c), which we will use for further investigation, other quantities like line center intensity (I_{center}), linear and circular polarization, and line width (FWHM) were computed. The quantities v_{Dopp} , I_{center} , and FWHM are inferred from a Gaussian fit to the four points in the line after they have been normalized using the continuum intensity at +227 mÅ. The velocity scale has been calibrated assuming a convective blueshift of 0.2 km s^{-1} at the disk center, and the absolute error in v_{Dopp} was estimated to be of the order of $\pm 0.2 \text{ km s}^{-1}$.

3. SOLAR OSCILLATIONS IN IMAx DATA

3.1. Acoustic Power

The two time series of the Doppler velocity measured by IMAx reveal a “flying shadow” pattern with a characteristic timescale of 5 minutes and a characteristic spatial length scale between 5'' and 10''. Such an animation will be a part of the electronic supplementary material of the introductory Letter by Solanki et al. (2010). This pattern is due to the solar f - and p -modes present on the Sun. The “flying shadows” originate from the stochastic superposition of a multitude of solar acoustic eigenmodes of various spatial wavelength, temporal frequency, and amplitude, which cause these “Five-Minute Oscillations.” For a quantitative analysis, we investigate the power distribution in the diagnostic diagram, where the spectral power density is displayed as a function of wavenumber k and temporal frequency ν ; see Figure 1. The frequency resolution in the Fourier domain is 0.52 mHz. We find a significant enhancement of oscillatory power between 2 and 7 mHz in the f - and p -mode areas. Ridges of solar acoustic oscillations are at best visible only in outlines at high wavenumber. The f -mode ridge seems to extend until a wavenumber of $\approx 5 \text{ Mm}^{-1}$, where the ridge is cut by the acoustic cutoff frequency at $\approx 5.3 \text{ mHz}$ (see Figure 1). The velocity of the superposition of f -modes has an rms amplitude of 147 m s^{-1} with a maximum velocity of 902 m s^{-1} . From the location of

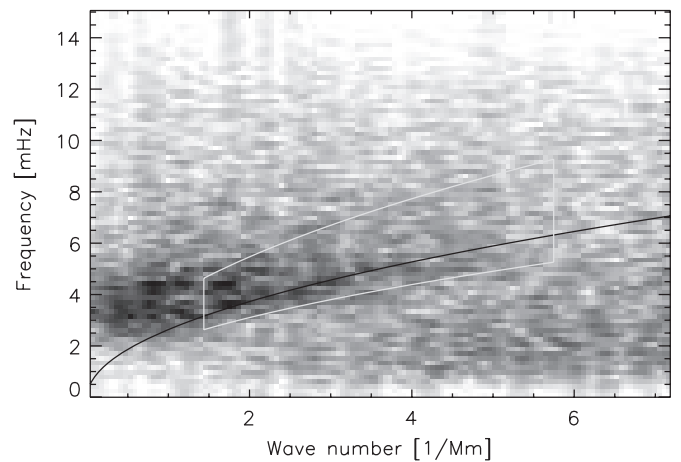


Figure 1. Spectral power density of the measured Doppler velocity as a function of wavenumber and frequency in arbitrary units. The color code reflects the mode energy: large amplitudes are coded dark and amplitudes compatible with zero are coded white. The black solid line indicates the theoretical position of the f -mode. The gray solid lines mark the borders of a Hanning bandpass filter, which is applied to the data.

enhanced power in this diagram, we conclude that besides the superposition of large-scale standing acoustic waves with low wavenumbers, the small-scale waves with high wavenumbers are also excited. These small-scale waves are expected to have a shorter lifetime than the large-scale waves. In the following, we will focus on the study of these small-scale oscillations. Before doing so, we would like to note that besides the sonic power we also find subsonic power below the f -mode. These subsonic velocities correspond to the convective granular motions that we observe.

3.2. Filter

We study the excitation and propagation of solar p -modes by first filtering the data. In order to remove trends in the time series a “first-difference” filter is applied. Further filtering for the f - and p_1 -modes is carried out in the Fourier domain. A fast Fourier transformation is applied to the time series. The result of this is multiplied by a filter that acts as a bandpass including the f -mode and the p_1 -mode ridges. Figure 1 outlines (gray lines) this three-dimensional filter as projection onto the $l-\nu$ diagram. The filter is based on Hanning windows with increasing widths as a function of the absolute magnitude of the wavenumber k . Further filter properties are that the filter allows only those modes with wavenumber $1.4 \text{ Mm}^{-1} \leq l \leq 5.7 \text{ Mm}^{-1}$ to pass, i.e., the filter removes the contributions of large-scale waves and subsonic granular motions. After filtering, the data are transformed back into the time domain. The resulting time series contains only the small-scale oscillatory motions.

3.3. Excitation and Propagation of Running Waves

The filtered data allow the excitation and propagation of small-scale acoustic waves to be seen. For a quick investigation, acoustic power maps are determined by averaging the square of the filtered velocity time series over time and at each pixel. Figure 2 displays this temporally averaged acoustic power of the oscillatory velocity field after filtering. In this map the granular network is visible, since the intergranular lanes and the borders of the granules exhibit strong acoustic power. However, there is also significant power present above the granules. This is visible in detail in the enlarged view shown

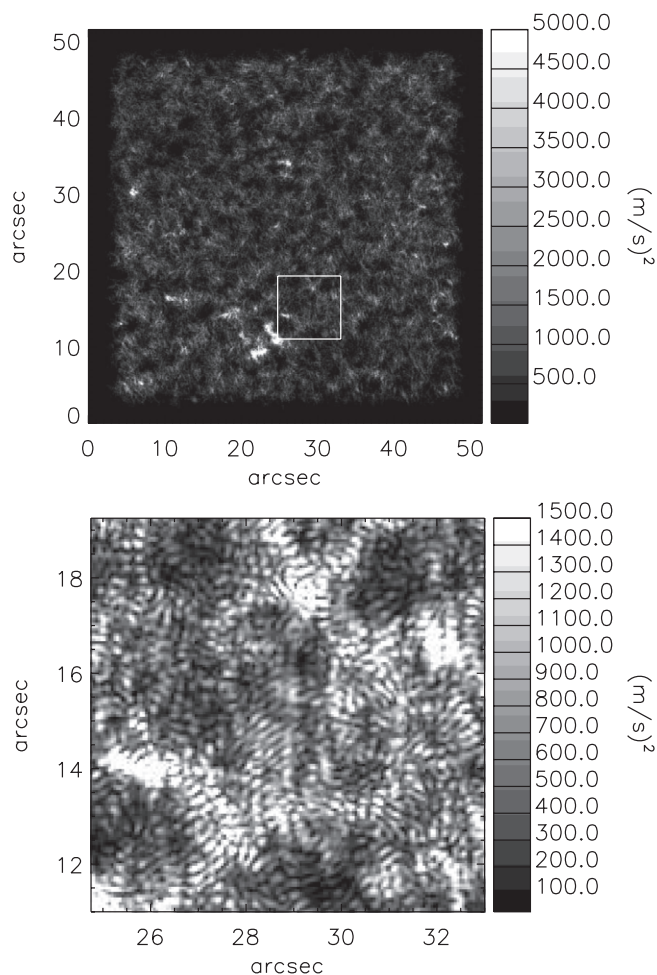


Figure 2. Acoustic power maps of the filtered data. White areas are locations on the Sun with high acoustic power. Top: average acoustic power of the whole FOV. Bottom: average acoustic power of an $8'25 \times 8'25$ section. The white rectangle in the top panel marks the area which is shown enlarged in the bottom panel. In the bottom panel only values below a threshold of $1500 \text{ (m s}^{-1}\text{)}^2$ are shown to make the acoustic power above the granules visible.

in the bottom panel of Figure 2. Inspecting the complete series of Doppler maps, the origin of this acoustic power enhancements on top of the granules are oscillations which are either excited in the intergranular lanes propagating through the granules or waves which are excited inside splitting or exploding granules.

A time sequence of such an exploding granule is shown in Figures 3 and 4. During the observation, the displayed granule continues to grow within the first half of the sequence before it fragments in the second half. Already at the beginning of the recording ($t = 199 \text{ s}$), parallel wave fronts are rippling on top of the granule. Surprisingly, these wave fronts are aligned with an intergranular lane that is forming during the sequence but finally splits the granule 265 s later ($t = 464 \text{ s}$). Further splittings of the granule occur at later times which seem to excite additional wave fronts on a smaller scale. Such events happen in multitude in the recorded time series and not only at this particular location. Based on a wavelet analysis, Bello González et al. (2010) study the distribution of acoustic power in space and time. They also find increased power above small fast-evolving granules, splitting granules, dark dots, and forming intergranular lanes.

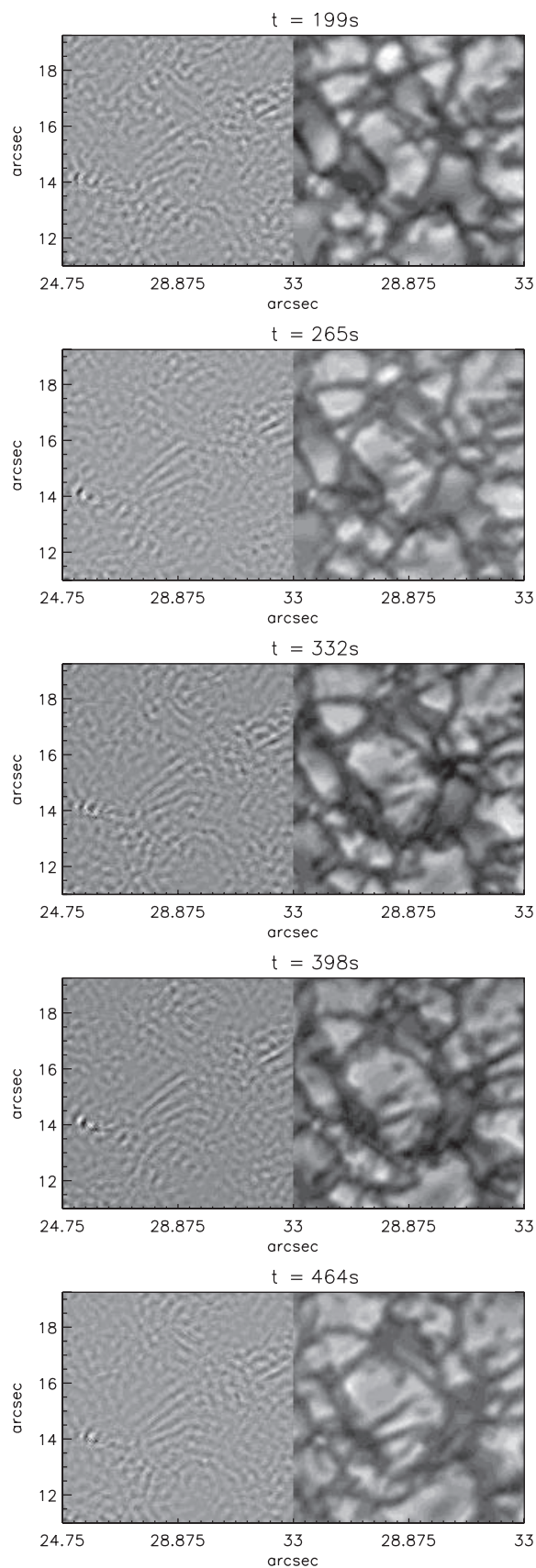


Figure 3. Time sequence of the filtered velocity time series (left) and the synchronously recorded continuum images of the same area (right). The snapshots are separated by 66 s. The exploding granule is located in the center. The spatial extent of this area is $8'3 \times 8'3$. The displayed area corresponds to the map shown in the bottom panel of Figure 2. The series is continued in Figure 4.

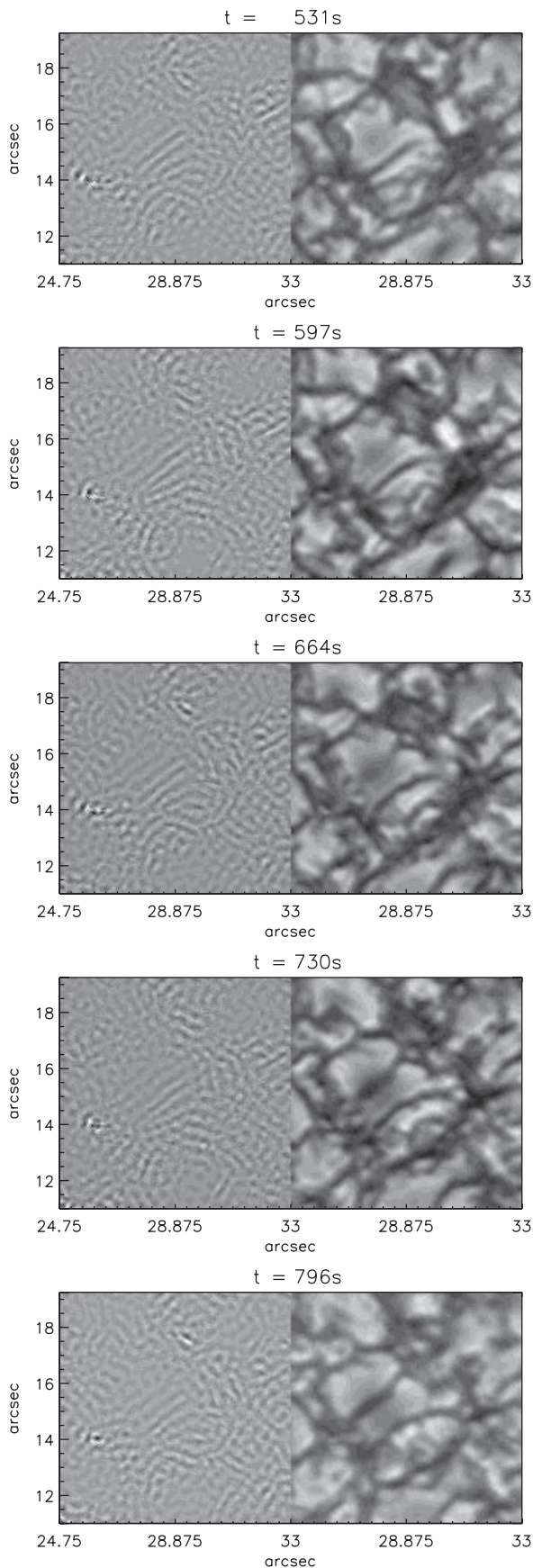


Figure 4. Continuation of the time sequence shown in Figure 3.

Another finding, which can be observed in all granules of Figures 3 and 4, is that the wave amplitude itself is attenuated in the granules. The centers of stable granules show only weak small-scale oscillatory motions. After approximately four wavelengths the high-degree oscillations are damped away. Therefore, waves excited in the intergranular lanes or in the splitting process of granules seem to lose energy while probing a granule. This might explain the comparatively high acoustic power along the borders of the granules.

4. CONCLUSIONS

We have investigated the properties of small-scale solar p -modes as recorded by the IMAx instrument during the flight of the balloon-borne SUNRISE observatory in 2009 June. We analyzed the Doppler velocity and continuum intensity observations to study the potential of such data sets for investigations of the excitation and propagation of high-degree acoustic waves on the Sun. Based on two sequences of data, we find that there is a strong relation between increased acoustic p -mode power with high wavenumber above granules and the onset of the splitting process that fragments granules. The splitting of granules triggers the excitation of waves several minutes before the actual splitting becomes visible in continuum radiation. A possible explanation for the excitation of such waves could be related to the formation of new intergranular lanes and connected turbulent motions which set off acoustic waves.

Therefore, we conclude that not only the vigorous motions in the established intergranular downdrafts are sources for acoustic waves, but also the processes related to the formation of new intergranular lanes. In future studies, e.g., based on either data from a second SUNRISE flight or from other instruments in space or on ground, we plan to investigate the excitation process of solar p -modes on the basis of spatially highly resolved data in greater detail. For a more quantitative analysis, we aim to obtain new contiguous observations that cover a longer time period, which shall allow us to resolve the ridges of the p -modes in the diagnostic diagram. Such longer time series are needed to measure, e.g., the Green's function, which is the response to an "acoustic event" on the Sun. This would help determining the statistical properties of the solar oscillation's source function, which is needed as an input to sensitivity kernels as they are calculated, e.g., for local helioseismology. Furthermore, it remains an open task to study the damping, transmission, and refraction of solar p -modes in granules. Observations of such quality could be useful for such investigations and might allow one to obtain an acoustic image of the formation and the structure of granules.

The German contribution to SUNRISE is funded by the Bundesministerium für Wirtschaft und Technologie through Deutsches Zentrum für Luft- und Raumfahrt e.V. (DLR), Grant No. 50 OU 0401, and by the Innovationsfond of the President of the Max Planck Society (MPG). The Spanish contribution has been funded by the Spanish MICINN under projects ESP2006-13030-C06 and AYA2009-14105-C06 (including European FEDER funds). The HAO contribution was partly funded through NASA grant NNX08AH38G. M.R. acknowledges support from the European Helio- and Asteroseismology Network (HELAS) which was funded as Coordination Action under the European Commission's Framework Programme 6. This work has been partially supported by the WCU grant

R31-10016 funded by the Korean Ministry of Education, Science, and Technology.

REFERENCES

- Barthol, P., et al. 2010, Sol. Phys., in press (arXiv:1009.2689)
Bello González, N., et al. 2010, *ApJ*, 723, L134
Berkefeld, T., et al. 2010, Sol. Phys., in press (arXiv:1009.3196)
Birch, A. C., Kosovichev, A. G., & Duvall, T. L., Jr. 2004, *ApJ*, 608, 580
Gandorfer, A., et al. 2010, Sol. Phys., in press (arXiv:1009.1037)
Goldreich, P., & Keeley, D. A. 1977, *ApJ*, 212, 243
Goldreich, P., & Kumar, P. 1988, *ApJ*, 326, 462
Goode, P. R., Strous, L. H., Rimmele, T. R., & Stebbins, R. T. 1998, *ApJ*, 495, L27
Houdek, G. 2006, in Proc. SOHO 18/GONG 2006/HELAS I, Beyond the Spherical Sun, ed. K. Fletcher & M. Thompson (ESA-SP 624; Noordwijk: ESA), 28
Martínez Pillet, V., et al. 2010, Sol. Phys., in press (arXiv:1009.1095)
Nordlund, Å. 1985, *Sol. Phys.*, 100, 209
Rimmele, T. R., Goode, P. R., Harold, E., & Stebbins, R. T. 1995, *ApJ*, 444, L119
Samadi, R., Nordlund, Å, Stein, R. F., Goupil, M.-J., & Roxburgh, I. 2003, *A&A*, 404, 1129
Solanki, S. K., et al. 2010, *ApJ*, 723, L127
Stein, R. F., & Nordlund, Å. 2001, *ApJ*, 546, 585
Unno, W. 1964, Trans. Int. Astr. Un., XII(B), 555